An Electrochemical Impedance Spectroscopy Study on a Lithium Sulfur Pouch Cell

Stroe, Daniel Loan; Knap, Vaclav; Swierczynski, Maciej Jozef; Stanciu, Tiberiu; Schaltz, Erik; Teodorescu, Remus

Published in:
ECS Transactions

DOI (link to publication from Publisher):
10.1149/07212.0013ecst

Publication date:
2016

Document Version
Accepted author manuscript, peer reviewed version

An Electrochemical Impedance Spectroscopy Study on a Lithium Sulfur Pouch Cell

D.-I. Stroe[a], V. Knap[a], M. Swierczynski[a], T. M. Stanciu[a], E. Schaltz[a], and R. Teodorescu[a]

[a] Department of Energy Technology, Aalborg University, Aalborg 9220, Denmark

The impedance behavior of a 3.4 Ah pouch Lithium-Sulfur cell was extensively characterized using the electrochemical impedance spectroscopy (EIS) technique. EIS measurements were performed at various temperatures and over the entire state-of-charge (SOC) interval without applying a superimposed DC current. The obtained results revealed a high dependency of the pouch cell's impedance spectrum on the operating conditions. An equivalent electrical circuit was proposed to further analyze the results and to quantify the contributions of different resistances to the total impedance of the Li-S pouch cell at different SOCs and temperatures.

Introduction

The demand for high energy density batteries has increased in the last decade, driven mainly by e-mobility, consumer electronics and military applications. Even though, today's Lithium-ion batteries are characterized by high performance in terms of power capability, lifetime, and safety, their volumetric and gravimetric energy density still prevents their full market penetration (1), (2). Thus, a lot research is carried out to develop rechargeable batteries chemistries with higher energy densities, which would totally fulfill the requirements of the aforementioned applications. In this respect, Lithium-air and Lithium-sulfur batteries could theoretically deliver the step-change in energy density required by applications such as e-mobility (3).

Lithium-sulfur (Li-S) batteries represent a very promising battery energy storage technology because of their high theoretical specific capacity (i.e., 1675 mAh/g) and energy density (i.e., 2600 Wh/kg) (3), (4). Furthermore, the use of sulfur, which is non-toxic, environmentally benign, and naturally abundant, as a cathode active material might reduce the battery cost and environmental concerns (5). Nevertheless, because of their inherent polysulfide shuttle mechanisms, Li-S batteries are characterized by rapid capacity fade, high self-discharge rate, and poor coulombic efficiency (5), (6).

Therefore, in order to analyze and assess the feasibility of using this new battery chemistry in various applications and for the improvement of the chemistry, a comprehensive understanding of the static and dynamic behavior is required. Electrochemical impedance spectroscopy (EIS) represents a powerful and well-established technique used for modelling purposes and/or for investigating the physical and electrochemical processes inside Li-ion batteries (7), (8); more recently, the EIS technique was applied successfully for similar purposes to Li-S batteries, as well (5), (9).

In this paper, we performed an in-depth characterization and investigation of the impedance spectra of a 3.4 Ah Li-S pouch cell. The impedance spectra was measured at various temperatures and SOC levels using the EIS technique. Furthermore, and electrical circuit was used to further process and analyze the measurements results.

State-of-the-art

The EIS technique was used to study different aspects related to Li-S batteries, as reported in the available literature. Kolosnitsyn et al. have used the EIS technique in (10) to study the changes in the properties of Li-S cell components during both charging and discharging. They shown that due to lithium polysulfides dissolution, the electrolyte conductivity changes and that the electrolyte's properties greatly influence the rate of the electrochemical process at both sulfur and lithium electrodes. In a later study (11), the same authors have obtained the impedance spectra of a Li-S coin cell for a reduced frequency range (i.e., 0.035 – 5 Hz) and illustrated that the cell's ohmic resistance reaches its maximum at the inflection point between the high voltage and low voltage plateau. Deng et al. in (5) have analyzed the changes in the Li-S cell impedance spectra by performing EIS measurements on a fully charged cell at five different temperatures and at room-temperature for different SOC levels. Furthermore, they have investigated the capacity fade mechanisms during 20 cycles by monitoring the changes in the measured impedance spectra of the Li-S cell. Similarly, Canas et al. have measured the impedance spectrum of a Li-S coin cell by means of EIS at different SOC levels over 50 cycles (9); a complex electrical circuit was used to model the EIS results and to further analyze the obtained results. The EIS technique, combined with other material dedicated techniques such as XRD and SEM, was used in (12) to investigate the electrochemical reactions of a sulfur cathode during both charging and discharging.

All the aforementioned investigation were performed on laboratory developed Li-S coin cells. To the best of our knowledge, there are no literature available EIS studies performed on pre-commercial or commercial Li-S cells. In this work, we present an extensive EIS characterization of a pre-commercial 3.4 Ah Li-S pouch cell. Furthermore, we analyzed the changes occurred in the cell's impedance spectrum due to the change in the SOC level and temperature.

Experimental Set-Up

Li-S Battery Cell under Test

For this study a pre-commercial Li-S pouch cell manufactured by Oxis Energy was used. The main parameters of this Li-S battery cell are summarized in Table I.

TABLE I. Main electrical and thermal parameters of the Li-S battery cell.

Parameter	Value
Nominal Capacity	3.4 Ah
Nominal Voltage	2.05 V
Maximum Voltage	2.45 V
Minimum Voltage	1.5 V
Nominal Charging Current	0.34 A (1C-rate)
Nominal Discharging Current	0.68 A (2C-rate)
Temperature Operation Range	+5°C to +80°C

Experiment Description

In order to fully characterize the impedance spectra of the considered 3.4 Ah Li-S pouch cell, the EIS measurements were carried out over the entire SOC interval, form 0% to 100% with a 5% SOC resolution, and considering a broad range of temperatures, from 15°C to 45°C, according to the following procedure:

1. Relaxation of the Li-S pouch cell at 15°C for two hours, in order to ensure stable thermo-dynamic conditions;
2. One nominal cycle, in order to 'reset the history' of the battery cell:
    a. CC charge with 0.1 C-rate (i.e., 0.34A) until the end-of-charge voltage (i.e, 2.45V) is reached;
    b. Discharge with 0.2 C-rate (i.e., 0.68A) until the end-of-discahrge voltage (i.e., 1.5V) is reached;
3. Second nominal cycle, in order to determine the cell's capacity at the test temperature; the cell's capacity needs to be known for the upcoming steps
4. CC charge with 0.1 C-rate (i.e., 0.34A) until the end-of-charge voltage (i.e, 2.45V) is reached;
5. EIS measurement at SOC = 100%
6. Discharge the cell with 5% SOC by a current of 0.2 C-rate.
7. Relaxation of the Li-S battery cell for a period of 30 minutes or until a decrease higher than 0.6 mV in the open circuit voltage is observed (which is caused by the pronounced self-discharge rate of the Li-S cells at high SOC levels);
8. EIS measurement at the new established SOC level;
9. Repetition of the steps 6 – 8 for the remaining SOC levels, considering a 5% SOC resolution;
10. Repetition of the steps 1 – 9 for the 25°C, 35°C, 45°C;

During all the tests, the Li-S pouch cell was placed into a temperature chamber with controlled temperature environment. Furthermore, the aforementioned temperature values refer to the temperature of the cell, which was measured by mean of a Type-K thermocouple as illustrated in Fig. 1.

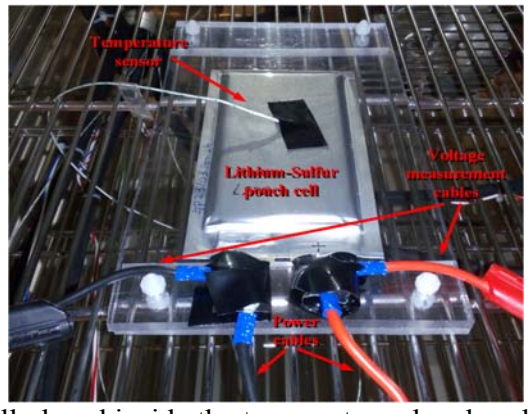

Figure 1. Li-S pouch cell placed inside the temperature chamber during the EIS characterization procedure

All the EIS measurements were performed in galvanostatic mode for a frequency sweep between 6.5 kHz and 10 mHz considering a total of 48 frequency points.

Furthermore during all the measurements no DC current was super-imposed on the small AC excitation signal.

Results

Li-S Battery Cell – Impedance Spectrum

Typical EIS Curve. A typical impedance spectrum of the considered 3.4 Ah Li-S pouch cell is presented in Fig. 2. As illustrated, the Nyquist curve is composed of a depressed semicircle in the high frequencies region (for this particular case 6.5 kHz – 27.4 Hz), a second depressed semicircle in the medium frequencies region (for this particular case 27.4 Hz – 0.11 Hz), and a straight line in the low frequencies region (for this particular case 0.11 Hz – 10 mHz). Furthermore, one can observe that the two depressed semicircles overlap each other.

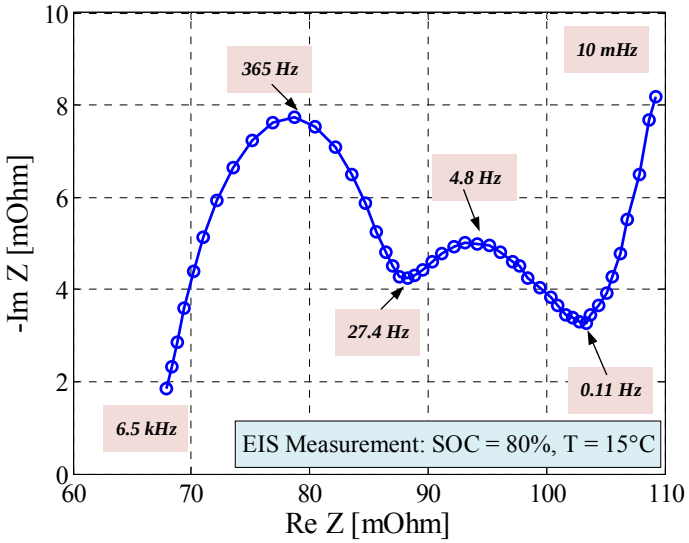

Figure 2. Typical Nyquist curve of the 3.4 Ah Li-S pouch cell.

Dependence of the Impedance Spectrum on the SOC. The impedance spectra of the Li-S pouch cell measured over the entire SOC interval at a temperature of 15°C (according to the procedure summarized in the previous section) is shown in Fig. 3. By analyzing the Nyquist curves illustrated in Fig. 3, two different trends were observed: for high SOC levels (i.e., in the interval 70% - 100% SOC), the impedance spectra shifts towards the right side of the Nyquist plane, while for low SOC levels (i.e., in the interval 0% - 65% SOC), the impedance spectra shifts towards the left side of the plane. This behavior is presented in Fig. 4 and Fig. 5. In (13) Knap et al., shown for a similar 3.4 Ah Li-S pouch cell that around 70% SOC is the inflexion point between the high voltage- and low voltage-plateau, which are characteristic for Li-S cells. Thus, the change in the shift of the impedance spectrum might be associated with the presence of the high and low voltage plateaus.

By analyzing the Nyquist curves presented in Fig. 4 and Fig. 5, one can observe that (except the case of 100% SOC), the diameter of the depressed semicircle corresponding to the high frequencies decreases with the decrease of the corresponding SOC value. On

the contrary, the diameter of the second depressed semicircle, which was obtained for the medium frequencies, is increasing with the decrease of the SOC.

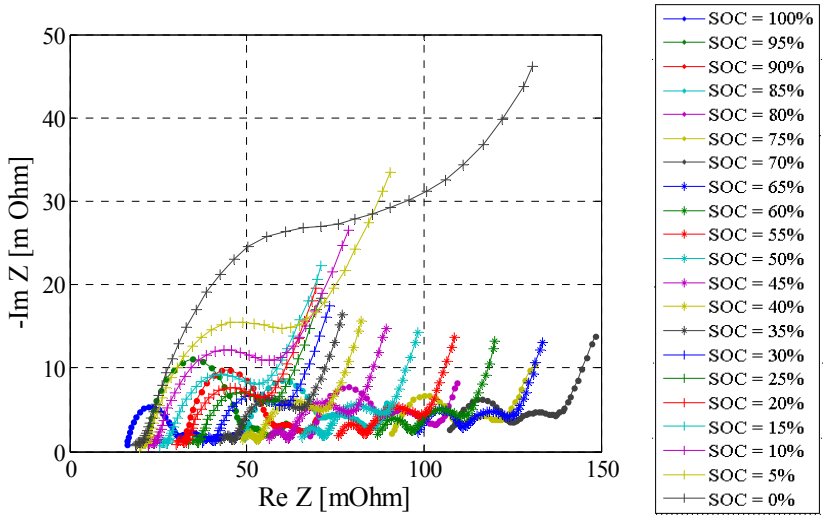

Figure 3. Impedance spectra of the Li-S pouch cell measured at 15°C

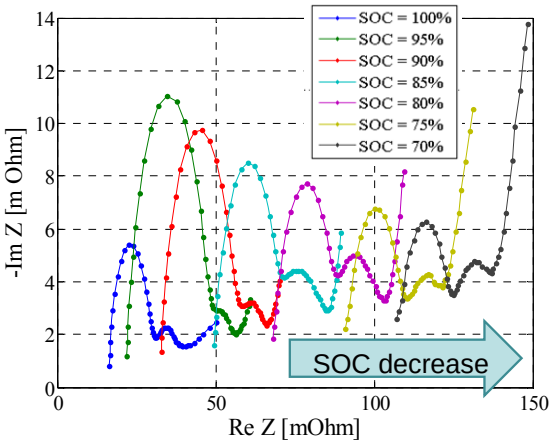

Figure 4. Impedance spectra of the Li-S pouch cell measured at 15°C and 70% - 100% SOC interval.

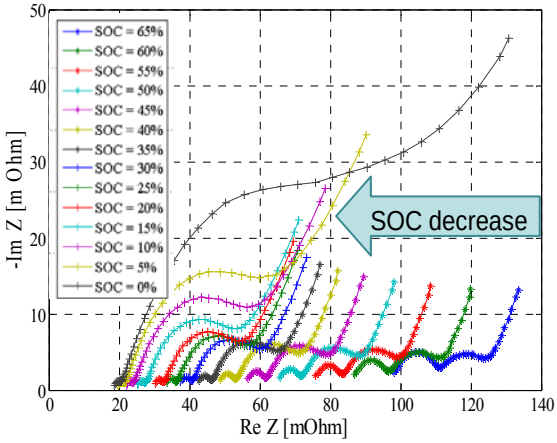

Figure 5. Impedance spectra of the Li-S pouch cell measured at 15°C and 0% - 65% SOC interval.

The impedance spectra of the Li-S pouch cell, which was measured at 25°C, 35°C, and 45°C are presented in Fig. 6 – Fig. 11. The trends that were mentioned for the impedance spectra obtained at 15°C are also valid for the other three considered temperatures. The only difference was observed for the value of the SOC where it occurs the change of the displacement of the Nyquist curves from the right side to the left side of the Nyquist plane: this behavior occurs at 75% SOC, 80% SOC and 85% SOC for 25°C, 35°C, and 45°C, respectively. Once more, this behavior might be associated with the decrease of the high voltage plateau of the Li-S pouch cell which takes place with the temperature increase; for example in (13), it is shown that for a cell temperature of 45°C, the shift between the high and low voltage plateaus occurs at approximately 82.5% SOC, while in this work, we observed the change in the EIS spectrum shift occurred for a SOC between 80% and 85% SOC.

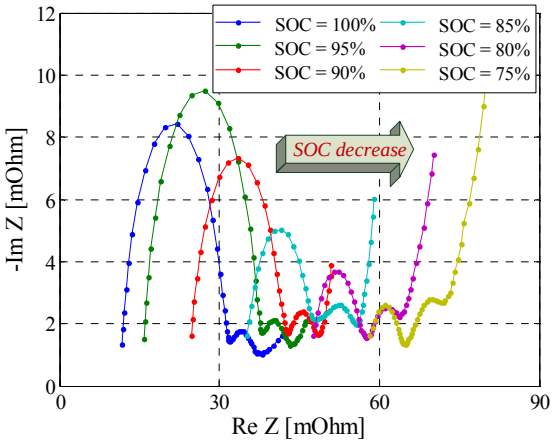

Figure 6. Impedance spectra of the Li-S pouch cell measured at 25°C and 75% - 100% SOC interval.

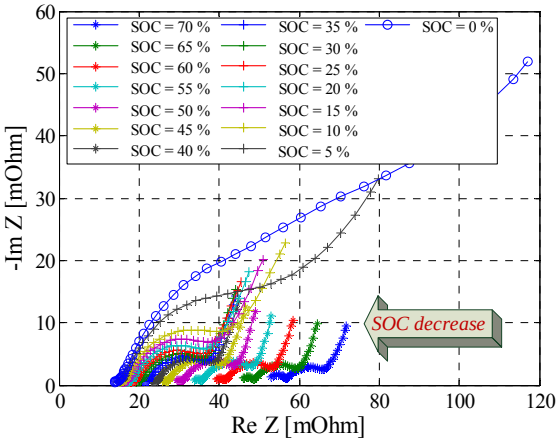

Figure 7. Impedance spectra of the Li-S pouch cell measured at 25°C and 0% - 70% SOC interval.

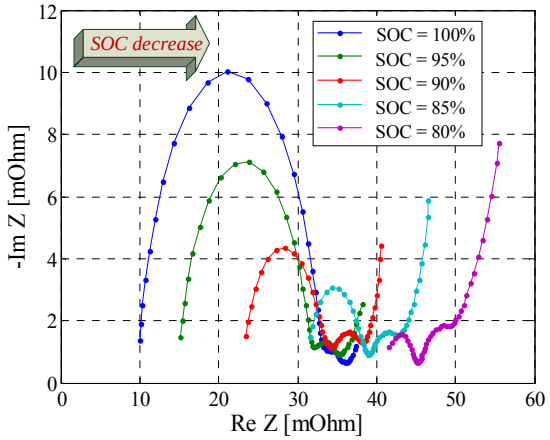

Figure 8. Impedance spectra of the Li-S pouch cell measured at 35°C and 80% - 100% SOC interval.

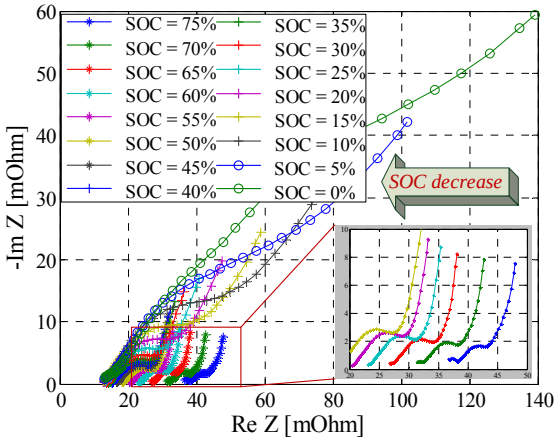

Figure 9. Impedance spectra of the Li-S pouch cell measured at 35°C and 0% - 75% SOC interval.

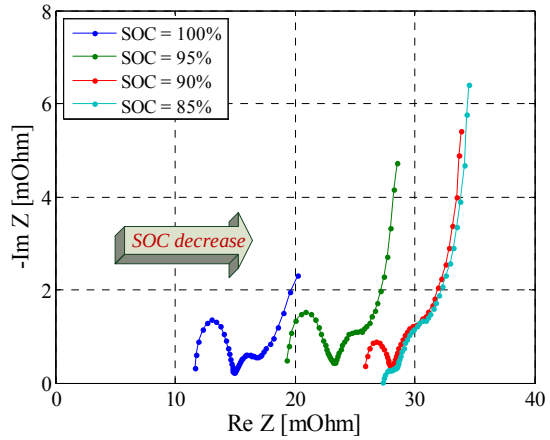

Figure 10. Impedance spectra of the Li-S pouch cell measured at 45°C and 85% - 100% SOC interval.

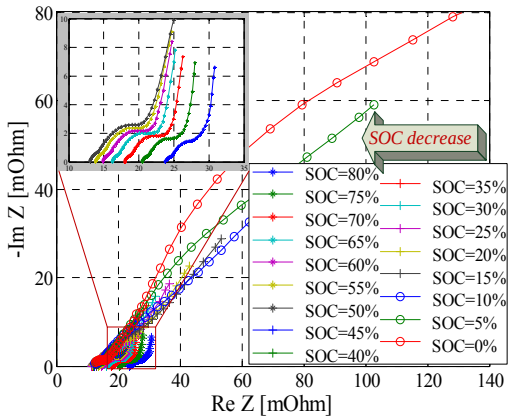

Figure 11. Impedance spectra of the Li-S pouch cell measured at 45°C and 0% - 80% SOC interval.

Dependence of the Impedance Spectrum on the Temperature. The change in the impedance spectrum of the considered Li-S pouch cell, which was caused by varying the cell temperature is presented in Fig. 12 for the case of 80% SOC. With the decrease of the temperature, it was observed a shift of the impedance spectrum towards the right hand side of the Nyquist plane; a similar behavior was presented for a laboratory-prepared Li-S coin cell by Deng et al. in (5). Furthermore, with the temperature increase, the diameter of the second depressed semicircle, corresponding to the medium frequencies, was reduced significantly, becoming almost indistinguishable for a temperature of 45°C. This decrease was as well presented in (5); however, in that case the behavior was not as pronounced as in our research. Finally, the first depressed semicircle was also influenced by the measurement temperature – with the temperature increase, a decrease of the dimeter of the semicircle was observed.

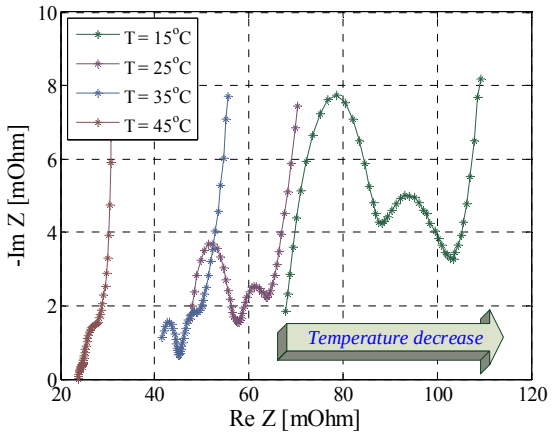

Figure 12. Impedance spectra of the Li-S pouch cell measured at 80% SOC and different temperatures.

Li-S Battery Cell – Equivalent Electrical Circuit

To better understand the dependence of the impedance spectrum on the SOC and temperature, the measured Nyquist curves were further processed by means of a curve fitting process.

Equivalent Electrical Circuit. Based on the shape of a typical Nyquist curve of the considered 3.4 Ah Li-S pouch cell (see Fig. 2), we have proposed the equivalent electrical circuit (EEC) presented in Fig. 13 to be used for the curve fitting process. The resistance Rs represents an ohmic resistance which sums the contribution from the electrolyte resistance and the resistance of the current collectors and cell connections (5), (9), (10). The first ZARC element (the parallel connection of the resistance R1 and constant phase element CPE1 (14)) models the high frequency semi-circle, while R2 and CPE2 were used to model the medium frequency semicircle. The diffusion of ions within the cathode, present at low frequencies, where modeled using a third ZARC element (composed of R3 and CPE3) (9). CPEs were used in the EEC instead of capacitors because of their better ability to approximate depressed semicircles, which were caused by the non-ideal behavior of the electrodes [2].

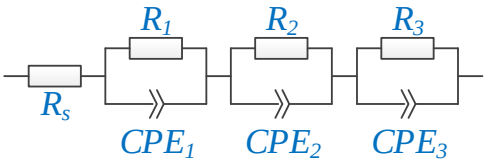

Figure 13. Equivalent electrical circuit of the 3.4 Ah Li-S pouch cell.

The suitability of the proposed EEC to fit the measured impedance spectra of the 3.4 Ah Li-S pouch cell is illustrated in Fig. 14. The accuracy of the fitting process was quantified using the normalized root mean square error (NRMSE).

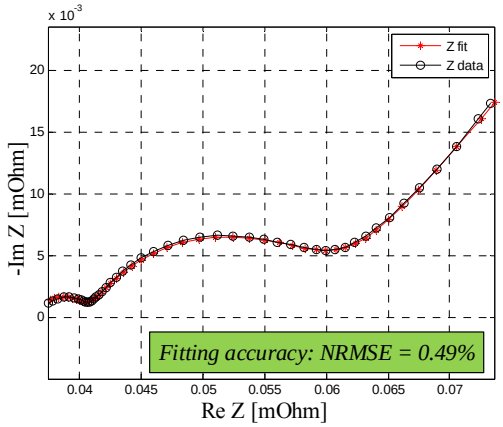

Figure 14. Curve fitting of the impedance spectrum measured at T = 15°C and SOC = 30%. Fitting accuracy: NRMSE = 0.49%. Extracted Parameters: Rs = 0.0364 Ω, R1 = 0.00425 Ω, Q1 = 0.1065 $\Omega^{-1}s^n$, n1 = 0.7851, R2 = 0.01933, Q2 = 7.1195 $\Omega^{-1}s^n$, n2 = 0.6889, R3 = 3.0691, Q3 = 218.211 $\Omega^{-1}s^n$, n3 = 0.5694.

Variation of the EEC Parameters with the Operation Conditions. The dependence of the resistance Rs (ohmic resistance), which was obtained from the fitting process, on the SOC and temperature is presented in Fig. 15. Independent on the Li-S cell temperature, the dependence of resistance Rs on the SOC follows two trends: the resistance increases with the SOC value until it reaches an inflection point from where it decrease steeply. A similar behavior of the resistance Rs was presented in literature (5), (9), (10). This inflection point changes monotonically with the temperature increase: for a temperature of 15°C, the inflection point was observed at 70% SOC, while for a temperature of 45°C, the inflection point was reached at 85% SOC. Furthermore, one can observe that the resistance Rs increases exponentially with the decrease of temperature. This process is caused by the decrease of the electrolyte ionic conductivity at low temperatures.

The change of the resistance R1 as function of SOC and temperature, as obtained from the curve fitting of the measured impedance spectra, are shown in Fig. 16. The resistance R1 increases exponentially with the increase in the SOC for all the four considered temperatures. Canas et al. reported in (9), a similar dependence of resistance R1 (which is defined in (9) as resistance R2) on the SOC for measurements carried out at room temperature. Furthermore, by performing dedicated tests, Canas et al, have related the resistance R1 with the charge transfer of sulfur intermediates at the cathode side (9).

Moreover, as illustrated in Fig. 16, the resistance R1 increases dramatically with the decrease of temperature; for example, at 60% SOC, the resistance R1 grows from 0.6 mOhm at 45°C to 10.2 mOhm at 15°C. The variation of resistance R2 as function of SOC for different temperatures is presented in Fig. 17. This resistive component of the EEC, decrease steeply with the increase of the SOC, independent on the considered temperature. A quasi-similar dependence was reported in (9), for a resistance denoted "R3" which was associated with the formation and dissolution of the S_8 and Li_2S compounds. For all the considered temperatures, the highest values of R2 were obtained for a discharged LiS battery cell when the accessible S_8 compound is not available; on the contrary, resistance R2 reaches its lowest values at high SOC values where sulfur dissolution occurs (9). Furthermore, for resistance R2 a reduced dependence on the temperature was observed, especially for SOC values higher than 20%. The dependence of the resistance R3 as function of SOC and temperature is shown in Fig. 18. Nevertheless, for this resistance, which is associated with the diffusion process, the fitting process has returned scattered values. Therefore, a clear conclusion regarding the variation of resistance R3 with temperature and SOC could not be drawn.

The dependence on SOC and temperature of the remaining parameters of the EEC, which are the generalized capacitances Q1, Q2, and Q3 and the depression factors N1, N2, and N3 were not analyzed.

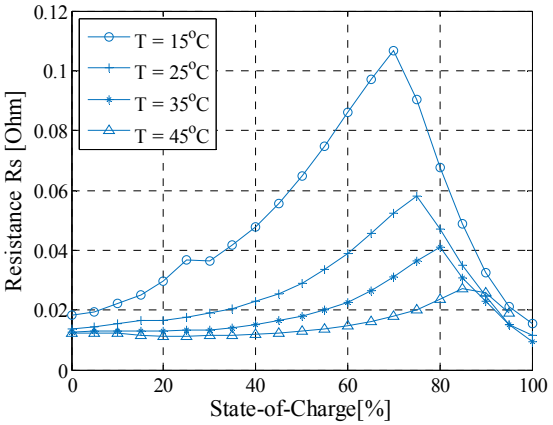

Figure 15. Variation of resistance Rs with SOC and temperature.

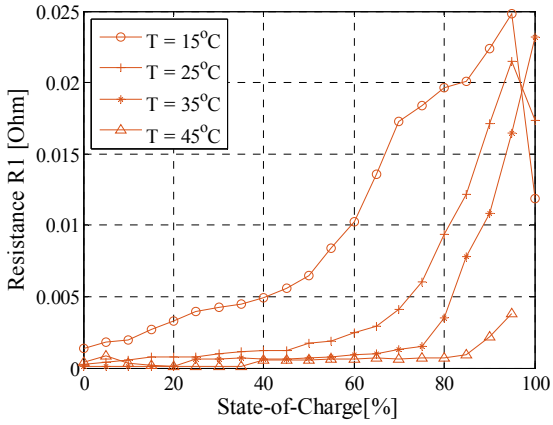

Figure 16. Variation of resistance R1 with SOC and temperature.

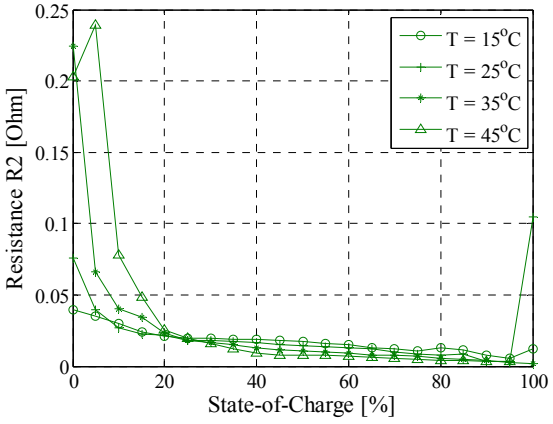

Figure 17. Variation of resistance R2 with SOC and temperature.

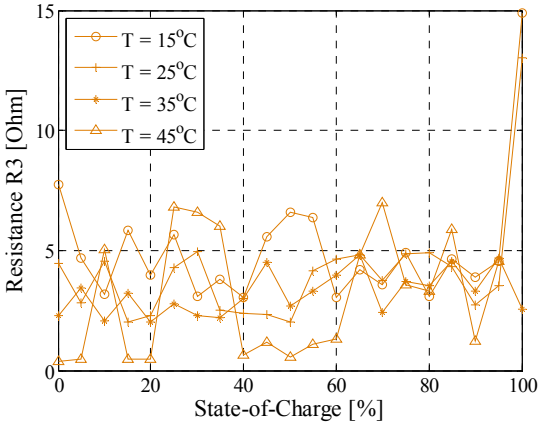

Figure 18. Variation of resistance R3 with SOC and temperature.

Conclusions

In this work, an extensive EIS characterization was performed for a 3.4 Ah Li-S pouch cell. EIS measurements were performed in galvanostatic mode, over the entire SOC interval at four different temperatures (i.e., 15°C, 25°C, 35°C, and 45°C); moreover, no superimposed DC current was applied during the EIS measurements. The obtained Nyqusit plots have shown a strong dependence on the SOC. This dependence was observed at all the temperatures. Furthermore, we have proposed an EEC – composed of a series ohmic resistance and three ZARC elements – that was used to curve fit the measured impedance spectra of the Li-S pouch cell. The results obtained from the curve fitting processes have shown different dependences of the EEC's elements on SOC and temperature. The ohmic resistance Rs has increased dramatically with the decrease in temperature and has reached its highest value at the SOC point which describes the transition between the high and low voltage profiles. Resistance R1, which in the literature is associated with the charge transfer process, shown an exponential increase with the decrease in temperature and with the increase of the considered SOC value. Furthermore, independent on the temperature, the resistance R2 decreases steeply until 20% SOC is reached; after this point, the value of resistance R2 decreases very slow and is almost not influenced by the temperature.

Acknowledgments

This work has been part of the ACEMU-project (1313-00004B). The authors gratefully acknowledge the Danish Council for Strategic Research and EUDP for providing financial support and would like to thank OXIS Energy for supplying the Lithium-Sulfur battery cells, which were used in this research.

References

1. J. B. Goodenough and K.-S. Park, *J. Am. Chem. Soc.*, **135**(4), 1167–1176 (2013).
2. B. Scrosati and J. Garche, *J. Power Sources*, **195**, 2419-2430 (2010).
3. P. G. Bruce, L. J. Hardwick, and K. M. Abraham, *MRS Bulletin*, **36**(7), 506-512 (2011).
4. X. Ji and F. Nazar, *J. Mater. Chem.,* **20**, 9821-9826 (2010).
5. Z. Deng et al., *J. Electrochem. Soc.*, **160**(4), A553 (2013).
6. D. Bresser, S. Passerini, and B. Scrosati, *Chem. Commun.*, **49**, 10545–10562 (2013).
7. D. Andre et al., *J. Power Sources*, **196**(12), 5349-5356 (2011).
8. Y.-C. Chang and H.-J. Sohn, *J. Electrochem. Soc.*, **147**(1), 50-58 (2000).
9. N. A. Canas et al., *Electrochmi. Acta*, **97**, 42-51 (2013).
10. V. S. Kolosnitsyn, E. V. Kuzimna, E. V. Karaseva, and S. E. Mochalov, *J. Power Sources* **196**(1), 1478-1482 (2011).
11. V. S. Kolosnitsyn, E. V. Kuzimna, and S. E. Mochalov, *J. Power Sources* **252**, 28-34 (2014).
12. L. Yuan, X. Qiu, L. Chen, and W. Zhu, *J. Power Sources* **189**, 127-132, (2009).
13. V. Knap et al., *J. Electrochem. Soc.*, **163**(6), A911 (2016).
14. E. Barsoukov and J. R. Macdonald, *Impedance Spectroscopy: Theory, Experiment, and Applications*, *2nd Edition*, Wiley, New York (2005).